Astronomy & Astrophysics manuscript no. h4195 February 2, 2008
(DOI: will be inserted by hand later)

NTT infrared imaging of star cluster candidates towards the central parts of the Galaxy. ⋆

C.M. Dutra[1,2], S. Ortolani[3], E. Bica[4], B. Barbuy[1], M. Zoccali[5] and Y. Momany[3]

[1] Universidade de São Paulo, Instituto de Astronomia, Geofísica e Ciências atmosféricas, CP 3386, São Paulo 01060-970, SP, Brazil

[2] Universidade Estadual do Rio Grande do Sul, Rua Bompland 512, São Borja 97670-000, RS, Brazil

[3] Università di Padova, Dept. di Astronomia, Vicolo dell'Osservatorio 2, 35122 Padova, Italy

[4] Universidade Federal do Rio Grande do Sul, Instituto de Física, CP 15051, Porto Alegre 91501-970, RS, Brazil

[5] European Southern Observatory, Karl-Schwarzschild-Strasse 2, D-85748 Garching bei München, Germany

Received ; accepted

Abstract. We address the issue whether the central parts of the Galaxy harbour young clusters other than Arches, Quintuplet and the Nuclear Young Cluster. A large sample of centrally projected cluster candidates has been recently identified from the 2MASS J, H and K_s Atlas. We provide a catalogue of higher angular resolution and deeper images for 57 2MASS cluster candidates, obtained with the near-IR camera SOFI at the ESO NTT telescope. We classify 10 objects as star clusters, some of them deeply embedded in gas and/or dust clouds. Three other objects are probably star clusters, although the presence of dust in the field does not exclude the possibility of their being field stars seen through low-absorption regions. Eleven objects are concentrations of stars in areas of little or no gas, and are classified as dissolving cluster candidates. Finally, 31 objects turned out to be the blend of a few bright stars, not resolved as such in the low resolution 2MASS images. By combining the above results with other known objects we provide an updated sample of 42 embedded clusters and candidates projected within 7°. As a first step we study Object 11 of Dutra & Bica (2000) projected at ≈ 1° from the nucleus. We present H and K_s photometry and study the colour-magnitude diagram and luminosity function. Object 11 appears to be a less massive cluster than Arches or Quintuplet, and it is located at a distance from the Sun $d_\odot \approx 8$ kpc, with a visual absorption $A_V \approx 15$.

Key words. Galaxy: open clusters and associations - ISM: dust, extinction

1. Introduction

The 2MASS Atlas (Skrutskie et al. 1997– http://pegasus.phast.umass.edu/2mass.html) has made it possible to study the infrared population of star clusters and candidates towards the central part of the Galaxy (e.g. Dutra & Bica 2000, 2001). By central part of the Galaxy we mean within 7° of the nucleus (1 kpc at the Galactic center distance). Recently, Portegies Zwart et al. (2001) modeled cluster formation and tidal survival in a more central region within 1.43° (200 pc).

The central part of the Galaxy is known to harbour the massive star clusters Arches, Quintuplet and the Nuclear Young cluster (e.g. Figer et al. 1999a, Gerhard 2001 and references therein). Several more may exist according to simulations by Portegies Zwart et al. (2001). They estimated 50 massive clusters within 200 pc, which would survive to a tidal dissolution time of ≈ 70 Myr. A fundamental question is whether clusters predicted by Portegies Zwart et al. (2001) can be detected. Can young clusters such as Arches and Quintuplet be detected not only within 200 pc but also up to 1 kpc? Are most central clusters too much absorbed to be seen at 2μm? The samples of Dutra & Bica (2000, 2001) provided candidates within both zones, which at the 2MASS angular resolution resembled the images of Arches and Quintuplet as seen on the same material. In the present study we employ larger resolution images to better select these samples, which is

Send offprint requests to: C.M. Dutra – dutra@astro.iag.usp.br

⋆ ESO proposals 67.B-0435 and 69.D-0225.

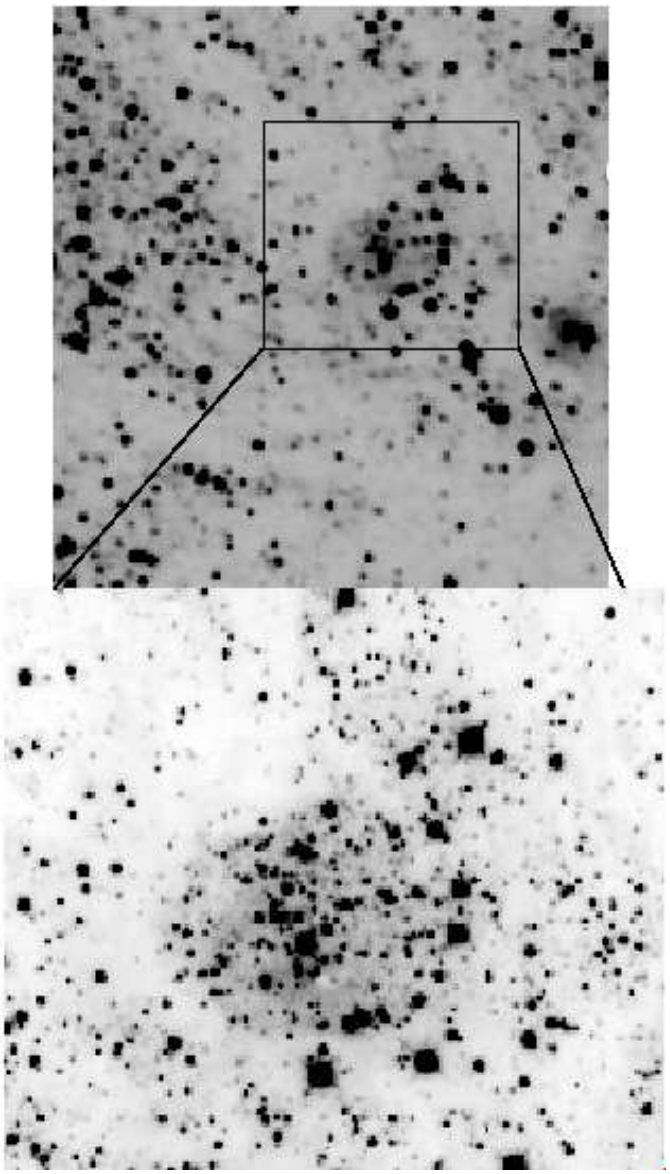

Fig. 1. Images of object 11: a $5' \times 5'$ K_S 2MASS extraction in the upper panel and a $2' \times 2'$ K_S SOFI large field extraction in the lower panel. North is up and west to the right.

important for detailed photometric studies with large telescopes.

Since star clusters towards the central parts dissolve in faster timescales, we would expect to observe objects at different dynamical stages and differently populated. Recently formed clusters will be embedded in the parent molecular clouds in different stages, and older objects unrelated to gas and dust may show evidence of advanced dynamical evolution.

Using the J, H and K_S 2MASS images, Dutra & Bica (2000, hereafter Paper I) detected 58 infrared star cluster candidates projected near the Centre. Typical dimensions were 1-2′, like those of Arches and Quintuplet. At higher resolution the Arches cluster is concentrated while the Quintuplet cluster is loose (Figer et al. 1999a). Seven additional candidates in the central parts were indicated by Dutra & Bica (2001, hereafter Paper II). The angular resolution of the 2MASS Atlas is not high, and it is necessary to increase it and obtain deep images in order to constrain the nature of the candidates. This is the objective of the present $K_{\rm s}$ survey with the 3.55 m ESO New Technology Telescope (NTT) making use of the resolving power of the SOFI camera to study 52 candidates from Paper I and 5 from Paper II. We also present detailed photometry of Object 11 from Dutra & Bica (2000).

In Sect. 2 we present the $K_{\rm s}$ survey and results. In Sect. 3 we present the H and K photometry of Object 11 and analyse the results. Finally, concluding remarks are given in Sect. 4.

2. A $K_{\rm s}$ survey of cluster candidates

In view of selecting the previous 2MASS samples for detailed studies with large telescopes we present a $K_{\rm s}$ imaging survey carried out with the NTT for 57 cluster candidates.

2.1. Observations and Reductions

We employed the SOFI camera at the NTT Nasmyth A focus with the detector Rockwell Hg:Cd:Te of 1024x1024 pixels (18.5 μm) Hawaii array. We used the Small Field mode ($2.47' \times 2.47'$ and scale $0.145''$/pixel) on June 27, 2001 and the Large Field mode ($4.94' \times 4.94'$ and scale $0.292''$/pixel) on July 4 - 6, 2002. The K_S band (2.162μm) allows one to minimize dust absorption effects ($A_{K_{\rm s}}=0.11A_V$, Cardelli et al. 1989). Owing to weather conditions only a few objects were observed on June 27, 2001 and July 5, 2002. In June 2001 we adopted a detector integration time DIT = 4 sec, a number of detector integrations NDIT = 5 and a number of exposures NEXP = 20, whereas on July 2002 DIT = 7, NDIT = 7 and NEXP = 18. More details on the observations are given in Table 1.

For infrared observations it is necessary to frequently subtract the sky thermal emission. We used the subtraction technique for small objects or uncrowded fields, from the SOFI Users Manual (Lidman et al. 2000). The reduction consisted of dark frame subtraction, sky subtraction and flat fielding, following the steps given in the SOFI manual.

In the process of flat fielding the illumination correction frames and the bad pixels maps, both available from the ESO webpages, were used.

2.2. Results

The higher angular resolution and depth of the NTT images with respect to the 2MASS Atlas allowed us to classify the objects more clearly now. Note that the classifications are based on eye estimates of the stellar overdensity on the images.

Table 1. Log of observations.

Date	Objects	Filter	Exposure	Seeing	Field
			(min.)	($''$)	
June 27 2001	3, 19, 24, 26, 01-40	H,K_s	6.7	1.5	Small
July 4 2002	1, 2, 4, 5, 6, 7, 8, 9, 10, 11, 12, 13, 14, 15, 16, 17, 20, 21,	K_s	14.7	0.8	Large
July 4 2002	22, 23, 25, 26, 29, 40, 41, 42, 43, 44	K_s	14.7	0.8	Small
July 5 2002	30, 31, 32	K_s	14.7	1.5	Large
July 6 2002	01-01,01-02,01-41,01-42, 33, 34, 35, 36, 37, 38, 39,	K_s	14.7	0.8	Large
July 6 2002	46, 47, 48, 49, 52, 53, 54, 55, 56, 57, 58	K_s	14.7	0.8	Large

Notes: Objects from Dutra and Bica (2001) are indicated by 01-, else from Dutra & Bica (2000).

2.2.1. Confirmed Clusters

Objects 11 (Fig. 1), 52 (Fig. 2a), 6 (Fig. 2b), 5 (Fig. 2b), 55, 10 (Fig. 2c), 01-40 and 01-41 (Fig. 2d) appear to be resolved star clusters, most of them embedded in nebulosity.

Objects 10 and 11 have counterparts in the Mid Space Experiment (MSX) survey (Egan et al. 1999). This infrared survey provides data and images in the bands A (8.28μm), C (12.13μm), D (14.65μm) and E (21.3μm) and is electronically available at the Web site http://irsa.ipac.caltech.edu/applications/MSX/. The infrared emission of Objects 11 and 10 in these MSX bands is probably due to dust heated by massive stars. In addition Object 10 has a counterpart in the IRAS point source catalog, [IRAS 17470-2853]. Using the colours diagram of IRAS PSC sources associated with ultra compact HII region from Wood & Churchwell (1989) and IRAS 17470-2853's 12μm, 25μm and 60μm IRAS fluxes, we find that it is an ultracompact HII region. In the field of Objects 11/10 there is diffuse emission with diameter $\approx 5'$ in a Digitized Sky Survey R band image (http://cadcwww.dao.nrc.ca/cadcbin/getdss), corresponding to the optical HII region Sh2-21 (Sharpless 1959). Using the 2MASS Atlas one can trace in the area a dust (molecular) cloud with a diameter of $\approx 15'$. These structures, if located at about the Galactic center distance, would define a giant molecular cloud and HII region with 2 embedded star clusters. In Sect. 3 we provide a NTT H and K photometry analysis of Object 11.

2.2.2. Possible Clusters

Objects 26 (Fig. 3a) and 56 (Fig. 3b) appear to be star clusters deeply embedded in dust and gas, in very early stages of star formation.

Near objects 12, 58 (Fig. 4a) and 01-42 (Fig. 4b) we find dust absorption. Therefore, it is not excluded that these objects are field stars seen through low absorption windows. Infrared colour-magnitude diagrams (CMD) may clarify the issue.

Object 01-01 (Fig. 4c) is an open cluster candidate. It is an interesting target for CMD studies, since not much is known about open clusters towards the Galactic center, a few kpc away from the Sun.

Object 49 is a clump of stars embedded in a nebula.

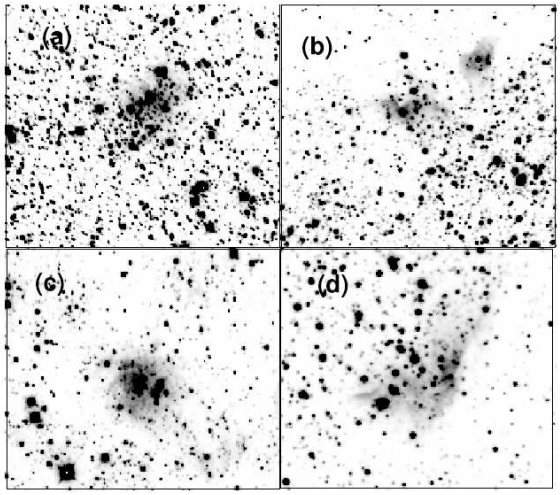

Fig. 2. K_s SOFI large field extractions: (a) $2' \times 2'$ of Object 52, (b) $2' \times 2'$ of Object 6 (centre) and Object 5 (right), (c) $2' \times 2'$ of Object 10, and (d) $2' \times 2'$ of Object 01-41. North is up and west to the right.

Several objects turned out to be concentrations of stars with little or no gas/dust in the area. They may be clusters in the process of dissolution. In the solar neighbourhood the timescale for dissolution of open clusters is a few Gyr or less and several have been studied in detail (Pavani et al. 2001, Carraro 2002, Pavani et al. 2003), while in the central 200 pc the timescale is reduced to $\approx$ 70 Myr (Portegies Zwart et al. 2001). These candidate dissolving clusters are objects 1, 7, 17, 25, 31, 32, 35, 40, 41, 42 and 01-02. Object 1 is shown in Fig. 4d.

2.2.3. Spurious Identifications

Based on NTT images, the following objects were found not to be clusters, but one or more relatively bright stars (plus faint ones) or clumps which were previously unresolved in the 2MASS images (Paper I). These are the objects 2, 3, 4, 8, 9, 13, 14, 15, 16, 19, 20, 21, 22, 23, 24, 29, 30, 33, 34, 36, 37, 38, 39, 43, 44, 46, 47, 48, 53, 54 and 57. Recording such blended images which mimic clusters is also important in view of future systematic cluster surveys on the 2MASS Atlas.

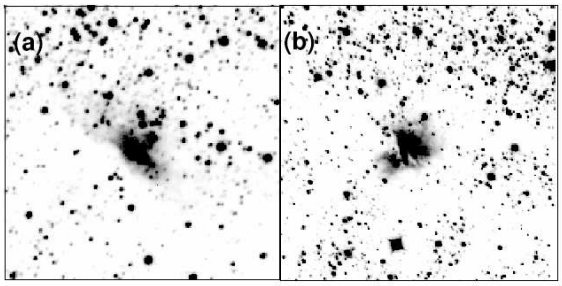

Fig. 3. K_s SOFI large field extractions: (a) $2' \times 2'$ of Object 26 and (b) $2' \times 2'$ of Object 56. North is up and west to the right.

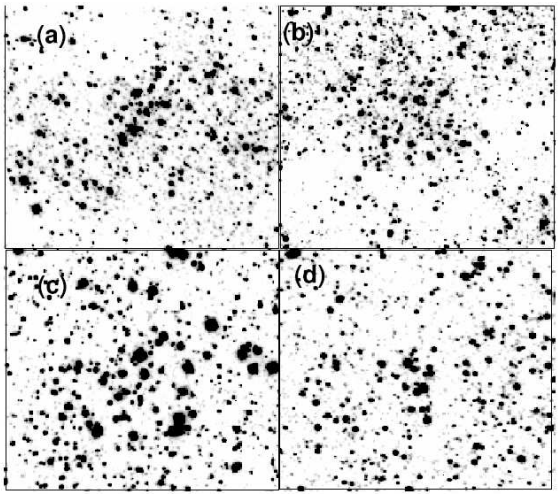

Fig. 4. K_s SOFI large field extractions: (a) $2' \times 2'$ of Object 58, (b) $3' \times 3'$ of Object 01-42, (c) $3' \times 3'$ of Object 01-01, and (d) $2' \times 2'$ of Object 1. North is up and west to the right.

2.2.4. Relation to nebulae

We checked the possibility of association of the present objects with optical and radio nebulae (e.g. Kuchar & Clark 1997; Caswell & Haynes 1987; Lockman 1989), which in turn reinforces the possibility that they are young stellar systems. Object 58 appears to be related to the optical HII region Sh2-17, Objects 5 and 6 to Sh2-20, and Objects 7, 10, 11 and 12 to Sh2-21. Although Object 01-01 is projected close to the dark nebula LDN74 (Lynds 1962), it appears to be an evolved open cluster and consequently unrelated to it.

Object 26 is related to the nuclear star-forming complex Sgr D and Object 52 to Sgr E (Liszt 1992). Object 01-40 is in the radio HII region G353.4-04, 01-41 in G354.664+0.470 and 01-42 in G359.3-0.3. Object 55 appears to be related to G359.54+0.18, and 56 to G359.7-0.4.

2.3. The updated sample of central clusters and candidates

We show in Fig. 5 the angular distribution including the results from the present survey. We indicate clusters, cluster candidates and cluster dissolution candidates. The overall sample spans objects within 7° (1 kpc at the Galactic Center distance), and we also indicate the region of 200 pc modeled by Portegies Zwart et al. (2001). In addition to objects from Dutra & Bica (2000, 2001) we show objects from a recent 2MASS cluster search in the directions of optical and radio nebulae (Bica et al. 2003). The asymmetry in the sense of more objects projected on the eastern part of the central Galaxy is due to the fact that the eastern side has been surveyed with 2MASS for infrared clusters in all directions (Dutra & Bica 2000), while the western side has been mostly surveyed for embedded clusters in the directions of nebulae.

Since we are dealing mostly with embedded clusters and candidates, these objects constitute an important sample for probing the cluster populations related to intervening spiral arms and the central parts of the Galaxy. We conclude that 42 objects are now available within 7° of the center, being 19 of them projected on Portegies Zwart et al.'s zone.

3. NTT H and K photometry of Object 11

The only object for which two colour photometry was available is Object 11 from Dutra & Bica (2000). It is located at $\approx 1°$ ($\ell = 0.58$, $b =$ -0.86) from the Galactic nucleus, thus projected on the zone modeled by Portegies Zwart et al. (2001). In this section we present a more detailed analysis of the cluster population, using its H, K_s CMD.

3.1. Infrared data

The H and K_s observations at the NTT were obtained with the SOFI camera equipped with the Hawaii 1024×1024 HgCdTe detector, with a pixel size of 18.5μm, on July 2002.

The observations used the SOFI small mode, with scale 0.145″/pixel and field $2.47' \times 2.47'$. The detector integration times DIT were 30 and 20 seconds for H and K_s, respectively. Similarly, the number of detector integrations NDIT was 2 and 3, for a total number of exposures NEXP of 15.

The thermal emission subtraction technique follows Lidman et al. 2000). The standard stars 9150, 9157 and 9170 from Persson et al. (1998) were observed at different airmasses. For each standard star five measurements of 2 sec for each airmass were obtained.

Dark frame subtraction, sky subtraction and flat fielding were applied. We used illumination correction frames

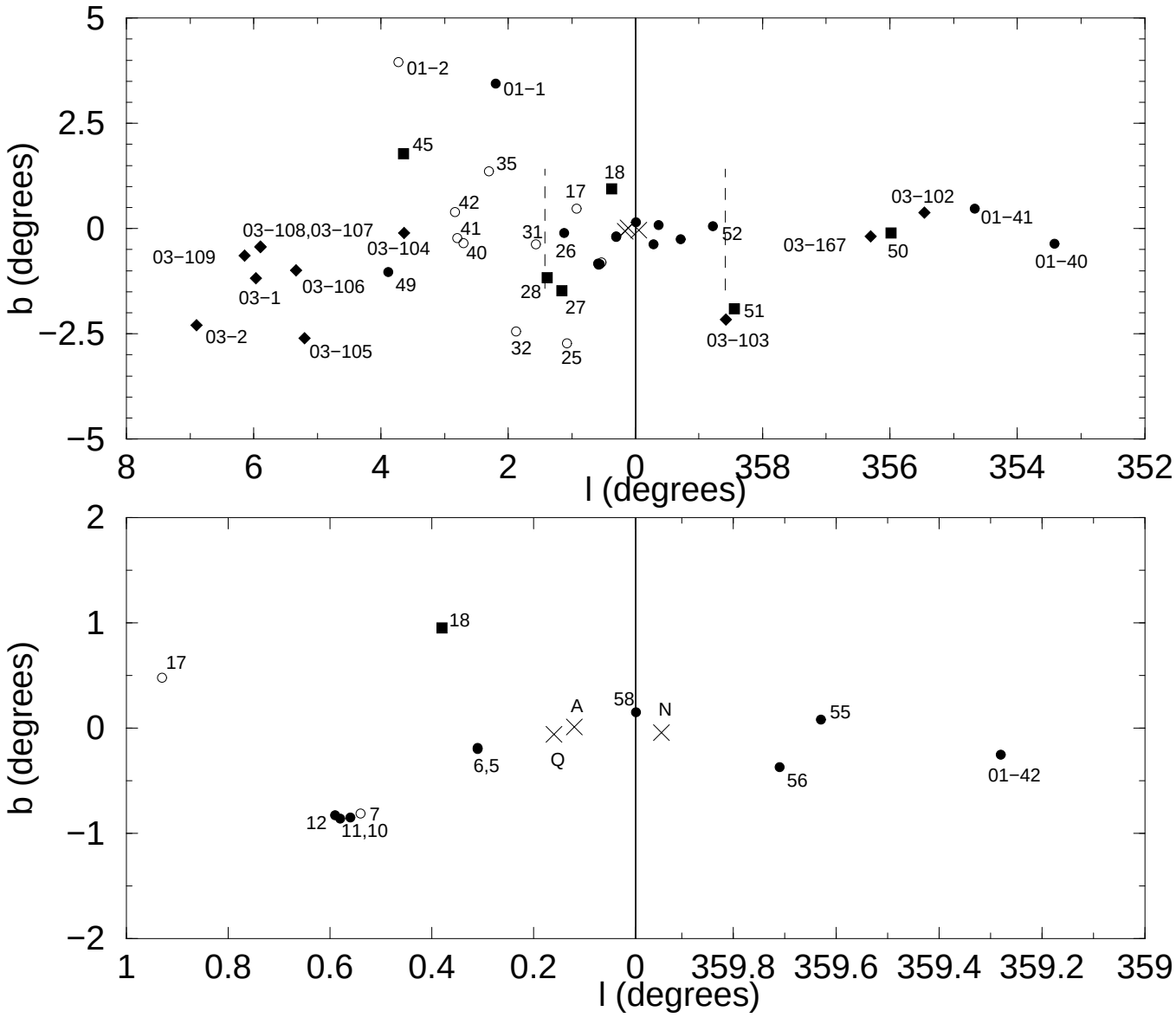

Fig. 5. Upper panel: updated angular distribution of star clusters and candidates in the inner 7° (1 kpc at the Galactic Center distance). Lower panel: blowup to show in detail the central region within 1°. Objects from Dutra & Bica (2001) are labeled as 01- and from Bica et al. (2003) as 03-, the other objects are from Dutra & Bica (2000). Crosses are the Arches, Quintuplet and Nuclear Young Cluster. Filled circles are objects from the present study which are confirmed as clusters or candidates. Open circles are dissolving cluster candidates. Filled squares are objects from Dutra & Bica (2000) not included in the present work. Filled diamonds are objects from Bica et al. (2003).

and the bad pixels masks, available from the ESO webpages for flat fielding.

We used a $K_{\rm s}$ filter, and we consider that this introduces an extra uncertainty in the K filter calibration of ± 0.02 mag (e.g. Ivanov et al. 2000). The instrumental magnitudes of the standard stars were normalized to 1 sec exposure and zero airmass, according to the following equation:

$$m^{'} = m_{\rm ap} + 2.5\,\log(t_{\rm exp}) - K_{\lambda}\,X \qquad (1)$$

where $m_{\rm ap}$ is the mean instrumental magnitude of the 5 measurements in a circular aperture of radius $R = 5.2$ arcsec, X is the mean airmass and $t_{\rm exp}$ is DIT in seconds. The mean extinction coefficients adopted for La Silla are: $K_H = 0.03$ and $K_K = 0.05$ (from ESO webpages). A least squares fit of the normalized instrumental magnitudes to the magnitudes of Persson et al. (1998) gave the following relations:

$$H - h_{\rm s} = -0.018 \times (H - K) + 22.920 \qquad (2)$$

$$K - k_s = -0.005 \times (H - K) + 22.35 \qquad (3)$$

The r.m.s. scatter of the residuals of the fit is 0.025 and 0.021 mag in H and K_s respectively. Together with

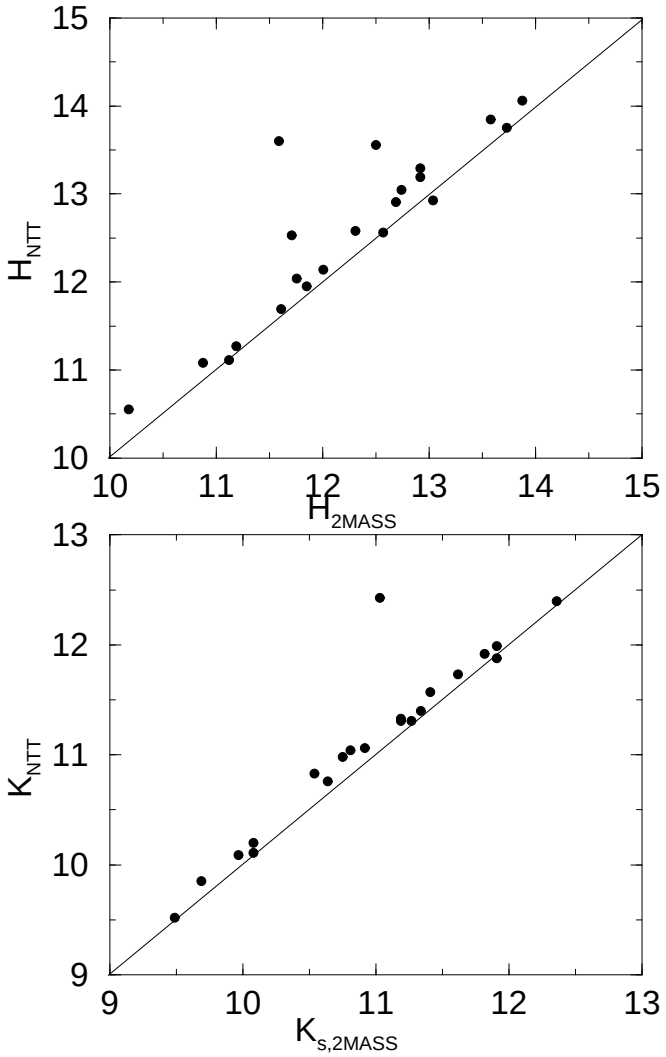

Fig. 6. H and K comparisons of the present and 2MASS photometries. Identity functions are shown.

the K_s to K filter, this yields total uncertainties of 0.025 and 0.041 in the H and K_s bands respectively.

The photometric extractions were performed on the stacked images using DAOPHOT/ALLSTAR package. The final calibrated magnitudes took into account aperture corrections applied to PSF magnitudes (0.115 and 0.080 mag for H and K_s respectively).

3.2. Comparison with 2MASS

We searched in our observations for stars in common with the 2MASS photometry. They occur both in the object area and in the surrounding field, reaching $H \approx 14$ and $K_s \approx 12.5$. The comparison is shown in Fig. 6. There is a linear relation between the photometries, which departs somewhat from identity. The zero-point differences between linear fits to the data and the identity function are 0.17 for H and 0.11 for $K - K_s$. In the linear fits we disregarded three deviant points in H and one in K which

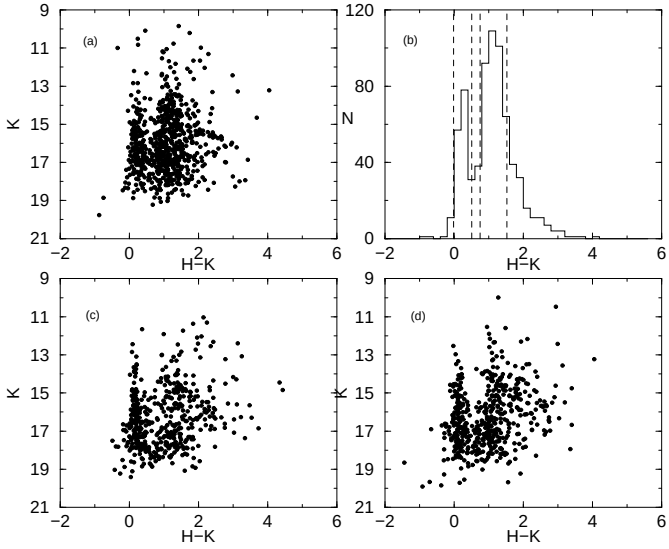

Fig. 7. $K, H-K$ diagrams for cluster (panel a) and fields 1 (panel c) and 2 (panel d) extractions. Panel b shows $H-K$ colour histogram for the object area.

are probably due to, e.g., crowding, cosmic rays or variable stars.

3.3. Analysis

For the photometric analyses we selected three $1.2' \times 1.2'$ square regions in the object area and two fields on either side to the east (Field 1) and west (Field 2).

Fig. 7 shows $K, H-K$ CMDs from the NTT photometry for the object (panel a) and the two side fields (panels c and d). In the CMDs two sequences are clearly present, which peak at $H - K \approx 0.25$ and 1.10 respectively, as shown in the colour histogram of panel b). Note that in the object CMD the second sequence is more populated than in the CMDs of the fields. In order to verify this point which would indicate the presence of a cluster, we built histograms of the distribution of stars along the K magnitude, assuming a $H-K$ colour interval for each sequence. Fig. 8 shows the results, where we assumed for the blue and red sequences the respective colour intervals $0.0 < H - K < 0.5$ and $0.75 < H - K < 1.5$. The upper panel of Fig. 8 shows that no contrast is observed for the blue sequence, indicating that we are dealing with field stars both in the object and field extractions. The middle panel of Fig. 8 shows a strong contrast between the object and field extractions for the red sequence, especially for stars fainter than $K = 13$, indicating a cluster. Finally, in the lower panel of Fig. 8 we show the field subtracted luminosity function which increases to $K \approx 16$, also suggesting a cluster. Completeness effects must be affecting fainter magnitudes.

For a more detailed CMD analysis we statistically decontaminated the cluster's CMD (Fig. 9a) from the Bulge stellar field contribution represented by stars extracted outside the cluster area (Fig. 9b). In the decontamination

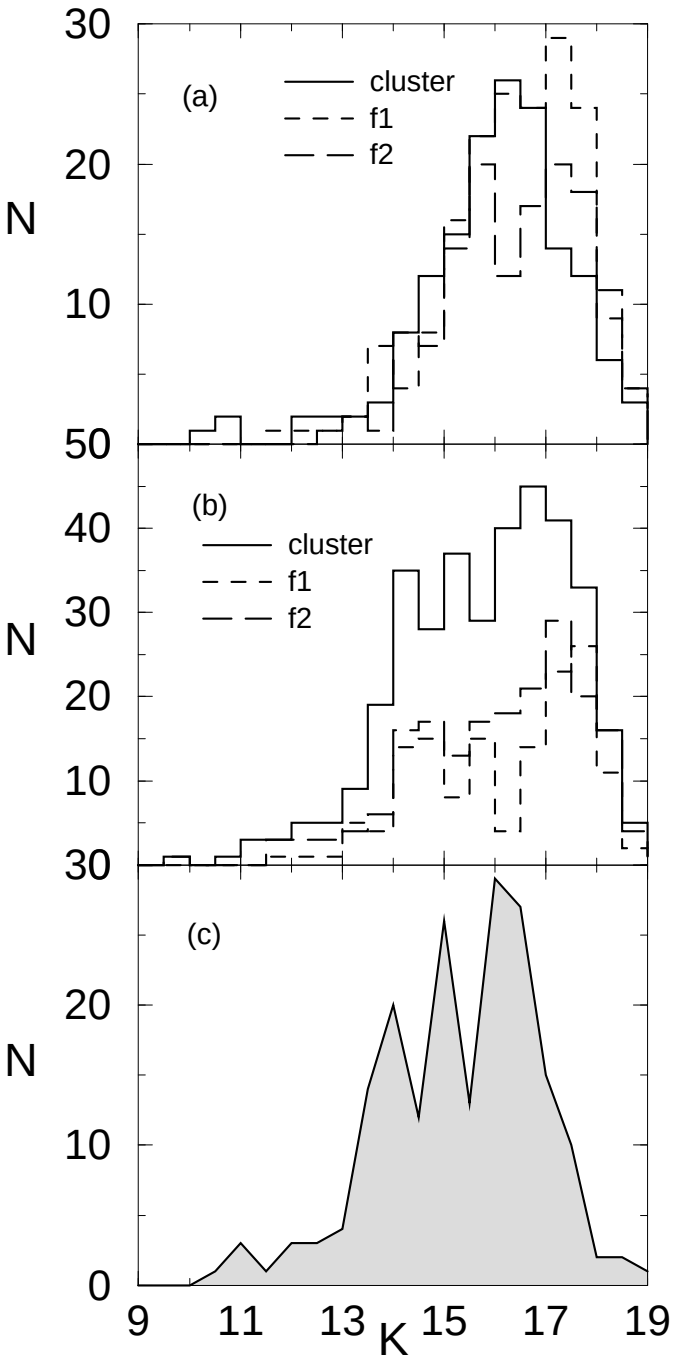

Fig. 8. Upper panel: K histogram for stars in the range $0.0 < H-K < 0.5$. Middle panel: K histogram for stars in the range $0.75 < H-K < 1.5$. Continuous line corresponds to object while dashed and long dashed lines to the fields. Lower panel: K cluster luminosity function derived from average field subtraction for $0.75 < H-K < 1.5$.

procedure, we scaled the Bulge stars contribution considering the cluster area. For each star in the scaled bulge CMD we picked the closest star in the cluster's CMD, and subtracted it. The distance on the CMD from bulge field star and star in the cluster area was defined as:

$$d = \sqrt{[7 \times \Delta(H-K)]^2 + \Delta H^2}$$

(see Zoccali et al. 2003, for more details about decontamination procedure). Figure 9c shows the decontaminated cluster CMD, while the CMD of the stars statistically removed from the cluster area CMD is shown in Fig. 9d.

The bulge tilted horizontal branch can be seen in Fig. 9b starting from $K = 13.8$ and $H-K = 0.76$. Assuming that the dust/molecular cloud must be behind the bulk of the bulge population seen in the diagram (it must have a much higher extinction), we can set a lower limit for the distance of Object 11. We use as reference for the bulge field population that of the CMDs at the minor axis b = -6° (Zoccali et al. 2003). In this field the bulge clump is located at $K = 12.7$ and $H-K = 0.25$. The reddening at -6° is $E(B-V) = 0.37$, corresponding to $E(H-K) = 0.10$ and $A_K = 0.175$. The intrinsic value is $K_0 = 12.53$, and $(H-K)_0 = 0.15$. The colour difference between the bulge in the direction of Object 11 and the -6° field is $\Delta(H-K) = 0.60$ corresponding to $A_K = 1.05$ (or $A_V = 9.6$). The relative distance modulus is $\Delta(m-M)_0 = 0.2$. Given the distance uncertainties this means that the two fields are at the same distance, i.e. compatible with that of the Galactic center. From the colour excess of the Object 11 field we get the minimum absorption which is likely the absorption in front of the cloud ($A_V = 9.6$). This value is consistent with the presence of an optical HII region (Sect. 2.2).

The 10^{th} brightest star method to determine cluster distances is useful when no spectral type information is available for young clusters (Dutra & Bica 2001). The method assumes similarity of luminosity functions of two clusters, and avoids uncertainties due to the brightest stars, for which luminosity effects are important. The 10^{th} brightest star in the giant H II region cluster NGC 3603 is an O4V star (Moffat 1983). We will make two assumptions, that Object 11 is: (i) a massive cluster where the 10^{th} brightest star is an O5V, or (ii) a less massive cluster where the 10^{th} brightest star would correspond to a B0V star. According to Cotera et al. (2000) O5V stars have intrinsic magnitude and colour $M_K = -4.81$ and $(H-K)_0 = -0.08$, while B0V stars have $M_K = -3.34$ and $(H-K)_0 = -0.07$.

Object 11 (Fig. 1) is embedded in nebulosity which suggests very young ages ($t < 5$ Myr). For the subsequent analysis we use Cotera et al.'s (2000) values for upper Main Sequence (MS) stars and the 10^{th} brightest star method to estimate the reddening and distance parameters for Object 11. We derive from Object 11's decontaminated CMD (Fig. 9c) a reddening $E(H-K) = 1.14$ with an important differential reddening $\delta E(H-K) = \pm 0.35$ as can be estimated from a mean reddening of $H-K = 1.07$ in comparison to Cotera et al.'s (2000) MS stars. Adopting the absorption ratios from Schlegel et al. (1998), one can derive the relation $A_K = 1.436E(H-K)$, which leads to $A_K = 1.64$. This value corresponds to a visual absorption $A_V \approx 15$.

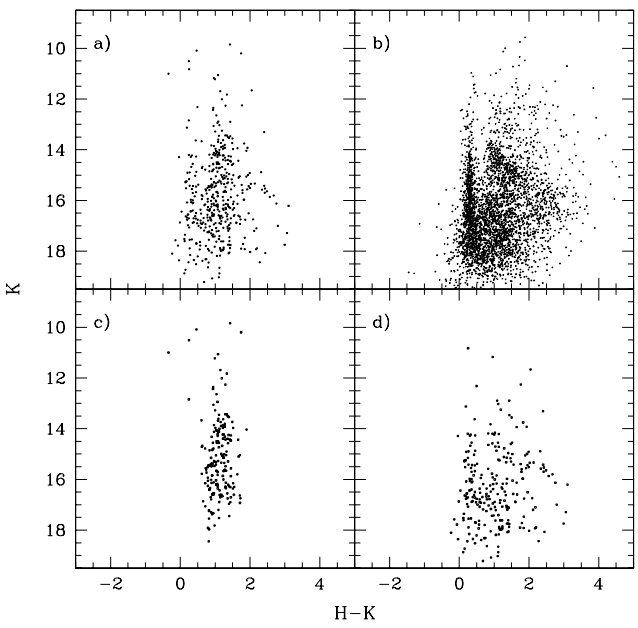

Fig. 9. $K, H-K$ diagrams: (a) Object 11 area, extraction of stars with distance $r < 43.5''$; (b) Bulge field, extraction of stars outside where field stars $r > 58''$; (c) clean cluster CMD; and (d) stars subtracted from the Object 11 area CMD in order to obtain the decontaminated CMD.

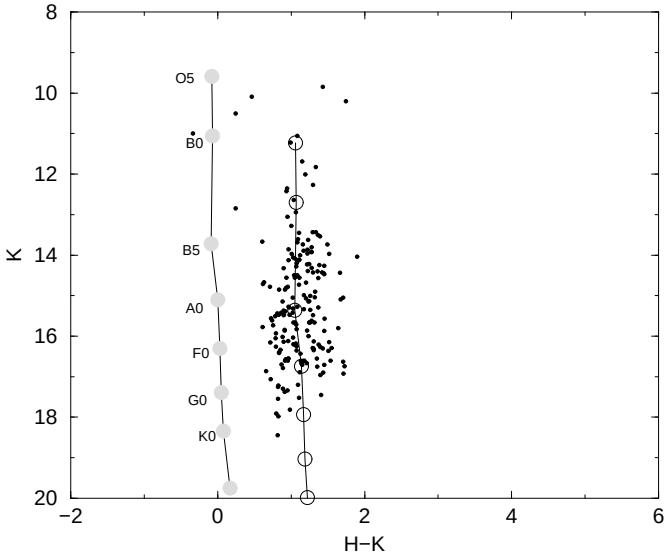

Fig. 10. $K, H-K$ diagram of object, where field stars have been statistically subtracted. MS spectral types sequence from Cotera et al. (2000): reddening-free and at 7.6 kpc (gray circles and solid line) and with a reddening/distance solution with $A_K = 1.64$ ($A_V = 15$) and $d_\odot = 7.6$ kpc (open circles and solid line).

According to Fig. 9c the 10^{th} brightest star in Object 11 is located at $K = 12.7$. Assuming Object 11 as a massive cluster similar to NGC 3603, we derive a distance from the Sun $d_\odot = 14.9$ kpc. On the other hand, we assume a less massive cluster with a B0V star as 10^{th} brightest, then $d_\odot = 7.6$ kpc. The Quintuplet cluster, argued to be at the Galactic centre distance, has $A_V = 29$ (Figer et al. 1999b), much higher than that of Object 11. Therefore, Object 11 appears to be slightly in the foreground of the Galactic centre, being a less reddened and less massive cluster, favouring the solution $d_\odot = 7.6$ kpc. Differential reddening is the main source of uncertainties in distance, assuming that the spectral type of the 10^{th} brightest star is correct. For Object 11 $\delta E(H-K) = \pm 0.35$ implies $\delta A_K = \pm 0.50$ and a distance uncertainty of $\pm$ 1.2 kpc. Figure 10 shows the decontaminated Object 11 CMD superimposed on Cotera et al.'s (2000) MS spectral type distribution considering the B0V reddening/distance solution. Note that we are probably reaching F0 stars. It would be important to carry out spectroscopy of cluster stars in order to further constrain the distance.

4. Concluding remarks

This study aimed to settle a star cluster sample for the exploration of the structure and star formation events towards the central parts of the Galaxy. By means of ESO NTT observations we increased the angular resolution and depth of observations for 57 infrared cluster candidates towards the central Galaxy, as compared to those of the 2MASS Atlas, where these objects had been first identified. We explored this sample showing which objects are clusters, remain as cluster candidates or appear to be dissolving cluster candidates. We also indicated additions from other samples giving an updated census of 42 objects within 7° (1 kpc distance from the Galactic centre), of which 19 are within 1.43° (200 pc). Detailed photometry of the present set of objects using large telescopes is required to derive their properties such as star membership, reddening and age, in order to establish their location in the Galaxy as intervening spiral arms or the Galactic Center.

We analyzed in detail one of these objects projected at $\approx 1°$ of the nucleus. H and K photometry of Object 11 showed a colour-magnitude diagram and luminosity function of a cluster. The cluster has $A_V = 15$ and appears to be located at $d_\odot \approx 8 \pm 1.2$ kpc from the Sun, therefore not far from the Galactic centre. The cluster appears to be less massive than the Arches and Quintuplet clusters.

Acknowledgements. We acknowledge support from the Brazilian Institutions CNPq and FAPESP. CMD acknowledges FAPESP for a post-doc fellowship (proc. 2000/11864-6). SO thanks the Italian Ministero dell'Università e della Ricerca Scientifica e Tecnologica (MURST) under the program on 'Stellar Dynamics and Stellar Evolution in Globular Clusters: a Challenge for New Astronomical Instruments'.

References

Bica, E., Dutra, C.M., Soares, J.B. & Barbuy, B., 2003, A&A, submitted.

Cardelli, J.A., Clayton, G.C. & Mathis, J.S. 1989, ApJ, 345, 245
Carraro, G. 2002, A&A, 385, 471
Caswell, J.L. & Haynes, R.F., 1987, A&A, 171, 261
Cotera, A.S., Simpson, J.P., Erickson, E.F., et al. 2000, ApJS, 129, 123
Dutra, C.M. & Bica, E. 2000, A&A, 359, L9
Dutra, C.M. & Bica, E. 2001, A&A, 376, 434
Egan, M.P., Price, S.D., Moshir, M.M., et al. 1999, The Midcourse Space Experiment Point source Catalog Version 1.2 Explanatory Guide, AFRL-VS-TR1999-1522, Air Force Research Laboratory
Figer D.F., Kim S.S., Morris M., et al. 1999a, ApJ, 525, 750
Figer D.F., McLean, I.S. & Morris, M. 1999b, ApJ, 514, 202
Gerhard, O. 2001, A&A, 546, L39
Girardi, L., Bertelli, G., Bressan, A., et al. 2002, A&A, 391, 195
Ivanov, V.D., Borissova, J. & Vanzi, L. 2000, A&A, 362, L1
Kuchar, T.A. & Clark, F. O. 1997, ApJ, 488, 224
Lidman, C., Cuby, J-G. & Vanzi, L. 2000, in "SOFI user's manual" Doc. No. LSO-MAN-ESO-40100-0003, issue 13
Liszt, H.S. 1992, ApJS, 82, 495
Lockman, F.J., 1989, ApJS, 71 469
Lynds, B.T. 1962, ApJS, 7, 1
Moffat, A.F.J. 1983, A&A, 124, 273
Pavani, D.B., Bica, E., Dutra, C.M., et al. 2001, A&A, 374, 554
Pavani, D.B., Bica, E., Ahumada, A.V., et al. 2003, A&A, 399, 113
Persson, S.E., Murphy, D.C., Krzeminski, W., et al. 1998, AJ, 116, 2475
Portegies Zwart, S.F., Makino, J., McMillan S.L.W., et al. 2001, ApJ, 546, L101
Schlegel, D.J., Finkbeiner, D.P. & Davis, M. 1998, ApJ, 500, 525
Sharpless, S. 1959, ApJ, 4, 257
Skrutskie, M., Schneider, S.E., Stiening, R., et al. 1997, in *The Impact of Large Scale Near-IR Sky Surveys*, ed. Garzon et al., Kluwer (Netherlands), 210, 187
Stetson, P.B. 1987, PASP, 99, 191
Stetson, P.B. 1994, PASP, 106, 250
Wood, D.O.S. & Churchwell E. 1989, ApJ, 340 265
Zoccali, M., Renzini, A., Ortolani, S., et al. 2003, A&A, 399, 931